

# New models on the ocean acoustic detection process

Harilaos N. Psaraffis and Anastassios N. Perakis

Department of Ocean Engineering, Massachusetts Institute of Technology, Cambridge, Massachusetts 02139

Peter N. Mikhalevsky

Naval Underwater Systems Center, New London Laboratory, New London, Connecticut 06320

(Received 10 December 1980; accepted for publication 10 March 1981)

The basic problem of the ocean acoustic detection process is formulated analytically under the assumption of fully developed saturated phase random multipath acoustic fluctuations. Detection is defined as occurring whenever  $\rho$ , the root-mean-square pressure at the receiver, exceeds a specified threshold level  $\rho_0$ . Two models, one exact and one approximate, are developed for obtaining the probability density functions of the time between two successive detections and of the time  $\rho$  is above  $\rho_0$  (holding time). The two models are compared with one another and with the extensively used  $(\lambda, \sigma)$  model. One of the reasons that the latter model has a limited success in practice is the inability to estimate the appropriate value for  $\lambda$ , a parameter which is determined empirically. In this paper we have derived an appropriate value for  $\lambda$ , in terms of  $\nu$  (the single path root-mean-square phase rate),  $\sigma_1^2$  (half the long time average mean-square pressure at the receiver) and  $\rho_0$  (the threshold level). Using this equivalent value for  $\lambda$ , we observe that our exact and approximate detection models exhibit similar long-term behavior but markedly different short-term characteristics as compared with the  $(\lambda, \sigma)$  model. This is due to the memory of the process, a property that cannot be accounted for in the  $(\lambda, \sigma)$  model. A comparison of these models with data obtained from various field experiments demonstrates, in most cases, an improved capability over the  $(\lambda, \sigma)$  model.

PACS numbers: 43.60.Cg, 43.30.Vh, 92.10.Vz, 43.30.Bp

## LIST OF SYMBOLS

$f_{x_1, \dots, x_n}(x_1, \dots, x_n)$	joint PDF of random variables $x_1, \dots, x_n$	$\lambda_2$	same as $\lambda_1$ , for $(\lambda, \sigma)$ model
$F(t)$	PDF of interarrival time (time between two successive detections)	$\nu$	root-mean-square single path phase rate
$H(t)$	PDF of holding time (time $\rho$ is above $\rho_0$ )	$\xi(t)$	per unit time conditional probability of a detection at time $t$ given a detection at time 0
$\text{prob}(\cdot)$	probability	$\rho$	root-mean-square pressure
PDF	probability density function	$\dot{\rho}$	$d\rho/dt$
$t, T$	time	$\rho_0$	detection threshold level for exact ("circle") model
$x$	cosine quadrature component of $\rho$ ( $= \rho \cos \phi$ )	$\sigma^2$	variance of the signal-to-noise ratio in $(\lambda, \sigma)$ model
$x_0$	detection threshold level for approximate ("square") model	$\sigma_1^2$	half the long time average mean-square pressure of the signal at the receiver
$y$	sine quadrature component of $\rho$ ( $= \rho \sin \phi$ )	$\Phi(\cdot)$	standardized normal cumulative density function
$\Lambda$	level in dB ( $= 10 \log_{10} \rho^2$ )	$\phi$	phase
$\dot{\Lambda}$	$d\Lambda/dt$	$\chi^2$	chi-square estimator
$\lambda$	$1/(\text{relaxation time})$ in $(\lambda, \sigma)$ model	$\psi(t)$	per unit time conditional probability of losing target at time $t$ given a detection at time 0
$\lambda_1$	unconditional probability of detection per unit time		

## INTRODUCTION

Much of the work in the area of acoustic detection in the ocean has traditionally been based on the so-called  $(\lambda, \sigma)$  model characterized by the "relaxation time"  $1/\lambda$  and the standard deviation  $\sigma$  of the "signal-to-noise ratio."<sup>1,2</sup> Use of this model relies heavily on parameter estimation from field experiments without application of the relevant physical and probabilistic structures of the process.

This situation has been improved recently by the efforts of several authors. The work of Dyer,<sup>3</sup> Dyer and Shepard,<sup>4</sup> Hamblen,<sup>5</sup> and Mikhalevsky<sup>6-9</sup> resulted in an increased comprehension of the fluctuation characteristics of underwater signals. Under the assumption of

a fully developed saturated multipath phase-random field, probability distributions for several random variables such as  $\rho$ ,  $\dot{\rho}$ ,  $\Lambda$ ,  $\dot{\Lambda}$ ,  $\phi$ , and  $\dot{\phi}$  (see symbol list) have been determined. In addition, many joint probability distributions have been derived.

The work described in this paper represents an attempt to apply the knowledge obtained by these recent findings in the area of ocean acoustic detection when the phase random multipath model applies. Specifically, the new knowledge of the probabilistic characteristics of acoustic fluctuations has enabled us to develop *two new detection models*, one exact and one approximate. The methodology used is essentially the same for the two models, the only difference between them being the

shape of the detection boundary in the quadrature components plane. It should be made clear that from a methodological point of view, the phase randomness assumption is not binding for the formulation of our detection models. The approach that will be presented sheds some light into the second-order statistics of a fading channel and is equally valid for any other explicitly defined probabilistic process for ocean fluctuations. For the purposes of this paper, we chose to apply our approach to the phase random model.

Defining detection events as upcrossings of the random variable  $\rho$  through a specified threshold level  $\rho_0$ , the exact model regards detection vents as outward crossings of the vector whose components are  $x = \rho \cos \phi$  and  $y = \rho \sin \phi$  (the quadrature components of  $\rho$ ), with the periphery of a circle of radius  $\rho_0$  centered at the origin of the  $(x, y)$  plane ( $\phi$ : phase). The approximate model replaces the circle with a square whose side is a function of  $\rho_0$ . The motivation for the development of the approximate model has been to increase computational efficiency with respect to the exact model.

In contrast to the  $(\lambda, \sigma)$  model, which is memoryless, both our models explicitly incorporate *memory characteristics*. As a result, the argument that it is very unlikely to have two detections separated by a very small time interval is demonstrated quantitatively. The same holds for the argument that two detections separated by a sufficiently long time interval are essentially uncorrelated. This is done by deriving expressions for the probability distributions of the time interval between two successive detections (subsequently referred to as the "interarrival time") and of the time interval for which  $\rho$  is above  $\rho_0$  (subsequently referred to as the "holding time"). The approach used for obtaining this derivation is essentially the same as that which was used successfully by Psaraftis<sup>10</sup> for a seemingly unrelated, yet strikingly similar problem (that of a ship slamming on a random sea surface).

It should also be emphasized at the outset that our definition of detection as an upcrossing of  $\rho$  implies that two successive detection events are separated by a time interval during which  $\rho \geq \rho_0$  (holding time) followed by loss of detection and by another time interval during which  $\rho < \rho_0$  (time to regain detection once holding is lost).

Our models are compared with fluctuations data available from Woods Hole and from the CASE experiment. Comparison with the data highlights the similarities and differences between the exact, the approximate, and the  $(\lambda, \sigma)$  models. In that respect the following conclusions seem important:

(1) One of the reasons that the  $(\lambda, \sigma)$  model has a limited success in practice seems to be the inability to estimate the appropriate value for  $\lambda$ , a parameter which is determined empirically. In this paper we have determined an appropriate value for  $\lambda$ , in terms of the single path root-mean-square phase rate  $\nu$ , the standard deviation  $\sigma_1$  of  $\rho$ , and the threshold level  $\rho_0$ . It should be made clear that all comparisons of the  $(\lambda, \sigma)$  model with our models and with data in this paper are

done using the above "equivalent" value for  $\lambda$ . The use of this "equivalent" value for  $\lambda$  instead of an empirical and arbitrary value is considered necessary if one is to perform a fair test of the  $(\lambda, \sigma)$  model with data.

(2) Both our models exhibit a short-term behavior markedly different from that of the  $(\lambda, \sigma)$  model. In that respect, it is shown that the detection process has *very strong* memory characteristics for short time intervals. For instance, our analysis demonstrates not only that it is very unlikely to have two detections very close to one another, but that the most probable time interval between two successive detections is, depending on the threshold level  $\rho_0$ , of the order of  $0.3/\nu$  to  $0.4/\nu$  (in seconds, if  $\nu$  is measured in Hz). Also, the most probable holding time is seen to be of the order of  $0.1/\nu$  to  $0.2/\nu$ . These results are in sharp contrast with the  $(\lambda, \sigma)$  behavior, (especially if  $\nu$  is small), where there is a finite likelihood for two detections to be separated by a very small time interval and where the most probable interarrival and holding times are (unrealistically) equal to zero.

(3) Both our models exhibit a long-term behavior similar to that of the  $(\lambda, \sigma)$  model. In that respect, two detections separated by a sufficiently long time interval are, as in the  $(\lambda, \sigma)$  model, uncorrelated. Furthermore, our quantitative analysis shows that the "decorrelation interval" (i. e., the interval above which no correlation between detections exists) is, in general, a function of the selected threshold level  $\rho_0$ , and of the order of  $0.4/\nu$  to  $0.6/\nu$ .

(4) The substitution of the circular detection boundary by a square represents a very good approximation. Thus the approximate model produces predictions which are essentially similar to those of the exact model and are obtained at a lower computational effort.

The paper is organized as follows:

Section I presents the analytical formulation of the detection problem under the assumptions of stationarity and phase randomness. Unconditional and conditional probabilities of detection are defined and their relation with the PDF's of the interarrival and holding times discussed.

Section II describes how these PDF's can be estimated from the conditional probabilities of detection.

Section III presents the application of this method to the case of the exact detection model, for which the detection region is a circle.

Section IV is devoted to a similar analysis concerning the approximate detection model for which the detection region is a square.

Section V briefly describes the currently used  $(\lambda, \sigma)$  model, and derives an appropriate value for  $\lambda$ .

Section VI presents some results of the comparison of our models, as well as the  $(\lambda, \sigma)$  model, with data.

Section VII provides a relative evaluation of all three models, and summarizes the main conclusions of this work.

## I. DETECTION PROBABILITIES: UNCONDITIONAL AND CONDITIONAL

In this paper, *detection at time  $t$*  is defined as an up-crossing event for random variable  $\rho$ , through a specified threshold level  $\rho_0$ , as follows:

$$\rho(t) = \rho_0, \quad \dot{\rho}(t) \geq 0. \quad (1)$$

An exactly equivalent criterion involves the random variable  $\Lambda = 10 \log_{10} \rho^2$ , stated as follows:

$$\Lambda(t) = \Lambda_0, \quad \dot{\Lambda}(t) \geq 0, \quad (2)$$

with  $\Lambda_0 = 10 \log_{10} \rho_0^2$ .

We first proceed to determine what we call the *unconditional probability of detection*, which we denote from now on as  $\lambda_1 dt$ . This is by definition the probability that (1) is satisfied at some instant of time in the interval  $(t, t+dt)$  where  $t$  is random and  $dt$  is small.

The evaluation of  $\lambda_1 dt$  is quite straightforward: Considering the interval  $(t, t+dt)$  we can say that (1) implies that  $\rho(t) \leq \rho_0$  and that  $\rho(t+dt) \geq \rho_0$ . Since  $dt$  is small,  $\rho(t+dt) \approx \rho(t) + \dot{\rho}(t)dt$ . Hence

$$\begin{aligned} \lambda_1 dt &= \int_{\rho=0}^{\rho_0} \int_{\dot{\rho}=\dot{\rho}_0}^{\dot{\rho}_0} f_{\rho, \dot{\rho}}(\rho, \dot{\rho}) d\rho d\dot{\rho} \\ &= dt \int_{\rho=0}^{\rho_0} \dot{\rho} f_{\rho, \dot{\rho}}(\rho_0, \dot{\rho}) d\dot{\rho}, \end{aligned} \quad (3)$$

where  $f_{\rho, \dot{\rho}}(\rho, \dot{\rho})$  is the joint PDF for  $\rho$  and  $\dot{\rho}$ . From Longuet-Higgins<sup>11</sup> and Hamblen<sup>5</sup> we have

$$f_{\rho, \dot{\rho}}(\rho, \dot{\rho}) = [\rho / (2\pi)^{1/2} \sigma_1^3 \nu] \exp(-\rho^2 / 2\sigma_1^2 - \dot{\rho}^2 / 2\nu^2 \sigma_1^2).$$

Substituting the above into (3) and performing the integration, we find that

$$\lambda_1 = [\rho_0 \nu / \sigma_1 (2\pi)^{1/2}] \exp(-\rho_0^2 / 2\sigma_1^2), \quad (4)$$

where  $\nu$  is in units of rad/s and  $\lambda_1$  is the average number of detections (or "arrivals") per unit time. This result was first obtained by Dyer and Shepard<sup>4</sup> and Mikhalovsky.<sup>9</sup>

From now on, we will call  $\lambda_1$  the "unconditional detection rate" or the "per unit time unconditional probability of detection." Relation (4) means that  $\lambda_1$  depends on the selected threshold level  $\rho_0$ , on  $\sigma_1^2$  and on  $\nu$ , in a Rayleighlike law.

In order to quantitatively examine the memory of the detection process, we proceed to examine what we call the *conditional probability of detection*, which we symbolize from now on with  $\xi(t)dt$ . This is by definition the probability that a detection occurs at some instant of time in the interval  $(t, t+dt)$ , given a detection occurred at time 0. It should be made clear that the above mentioned detection in  $(t, t+dt)$  is *not necessarily the first one* after the detection at time 0.

To evaluate  $\xi(t)dt$  we proceed as follows:

$$\begin{aligned} \xi(t)dt &= \text{prob}[\text{detection at } t_2 \in (t, t+dt) | \text{detection at } t_1 \in (0, dt)], \\ &= \frac{\text{prob}(\text{detection at } t_2 \text{ and detection at } t_1)}{\text{prob}(\text{detection at } t_1)}, \\ &= \frac{dt}{\lambda_1} \int_{\rho_1=0}^{\rho_0} \int_{\dot{\rho}_2=0}^{\dot{\rho}_0} \dot{\rho}_1 \dot{\rho}_2 f_{\rho_1, \rho_2, \dot{\rho}_1, \dot{\rho}_2}(\rho_0, \rho_0, \dot{\rho}_1, \dot{\rho}_2) d\dot{\rho}_1 d\dot{\rho}_2, \end{aligned}$$

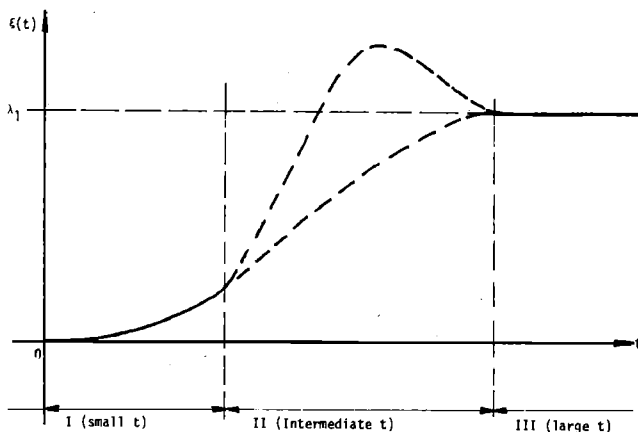


FIG. 1. Expected behavior of  $\xi(t)$ .

where  $f_{\rho_1, \rho_2, \dot{\rho}_1, \dot{\rho}_2}(\rho_1, \rho_2, \dot{\rho}_1, \dot{\rho}_2)$  is the joint PDF of  $\rho_1, \rho_2, \dot{\rho}_1, \dot{\rho}_2$  (subscripts 1 and 2 refer to times 0 and  $t$ , respectively). We then find that

$$\begin{aligned} \xi(t) &= \frac{1}{\lambda_1} \int_{\rho_1=0}^{\rho_0} \int_{\dot{\rho}_2=0}^{\dot{\rho}_0} \dot{\rho}_1 \dot{\rho}_2 f_{\rho_1, \rho_2, \dot{\rho}_1, \dot{\rho}_2}(\rho_0, \rho_0, \dot{\rho}_1, \dot{\rho}_2) d\dot{\rho}_1 d\dot{\rho}_2. \end{aligned} \quad (5)$$

From now on we will call  $\xi(t)$  the "conditional detection rate" or the "per unit time conditional probability of detection." Again, it should be made clear that  $\xi(t)$  is *not* a PDF.

We can evaluate  $\xi(t)$  according to (5) if the form of  $f_{\rho_1, \rho_2, \dot{\rho}_1, \dot{\rho}_2}$  is known. The corresponding analysis is presented in Secs. II and III, of the paper. For the moment, we present some qualitative arguments about the anticipated form of  $\xi(t)$ , arguments which will be seen to be confirmed by the quantitative analysis in later sections. To begin with we anticipate the existence of a "decorrelation time," which can be thought of as the time  $t_0$  following a given detection after which the conditional probability of detection equals the unconditional probability, or, in other words, the existence of a detection at time 0 does not affect the probability of a new detection at time greater than  $t_0$ . Therefore, as  $t \rightarrow \infty$ , we expect  $\xi(t) \rightarrow \lambda_1$  (Fig. 1). On the other hand we do not expect to have a second detection *immediately* after the first one, since *it will, in general, take a finite time* for our signal to drop below the threshold, and then rise above it again. Therefore it can be argued that  $\xi(t)$  will be very small as  $t \rightarrow 0$ , and this is also shown in Fig. 1. For intermediate values of  $t$ , the form of  $\xi(t)$  cannot be predicted by such qualitative arguments: Both shapes in Fig. 1 have been obtained for certain values of the threshold level, using our new detection models.

## II. PROBABILITY DISTRIBUTIONS OF THE INTERARRIVAL AND HOLDING TIMES

We will use the term "interarrival time" to denote the time between two successive detections. (For instance,  $t_{13}$  and  $t_{35}$  in Fig. 2.) The exact evaluation of the PDF of the interarrival time seems to be very difficult. Longuet-Higgins,<sup>11</sup> Rice,<sup>12</sup> and McFadden<sup>13</sup> have pre-

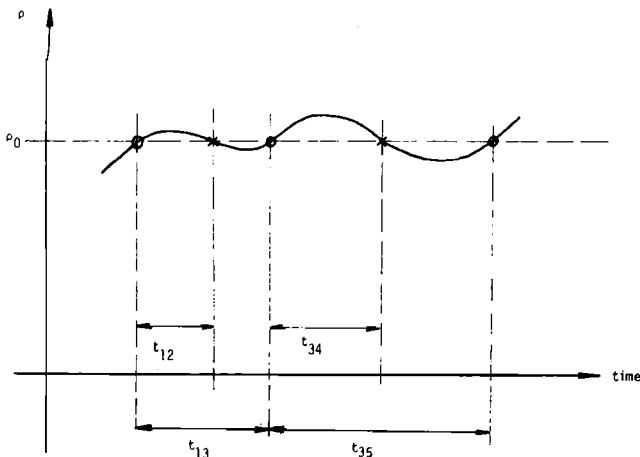


FIG. 2. Definition of interarrival and holding times.

sented several approaches to this problem in the general context of axis crossing of random functions. We propose here the technique used successfully by Psarafitis,<sup>10</sup> which states that a good way to approximate the above PDF is by the function

$$F(t) = \begin{cases} \xi(t) \exp\left(-\int_0^t \xi(x) dx\right), & t > 0, \\ 0, & t \leq 0, \end{cases} \quad (6)$$

where  $\xi(t)$  is obtained from (5).  $F(t)$  is different from  $\xi(t)$  in two respects: First,  $F(t)$  is a PDF whereas  $\xi(t)$  is not [ $\int_{-\infty}^{\infty} F(t) dt = 1$ , whereas  $\int_{-\infty}^{\infty} \xi(t) dt = \infty$ ]. Second,  $F(t)$  refers to the time between *two successive* detections, whereas  $\xi(t)$  refers to the time between *any two* detections. For small  $t$ ,  $F(t) \approx \xi(t)$ , because a detection which occurs within a very small interval after any given detection, is most likely to be the *first* one after that given detection. Equation (6) is consistent with this argument, since as  $t \rightarrow 0$ ,  $\int_0^t \xi(x) dx \rightarrow 0$  and hence  $F(t) \rightarrow \xi(t)$ .

We now define "holding time" to be the interval between any upcrossing through the threshold  $\rho_0$  and the first downcrossing through  $\rho_0$  that follows. (For instance,  $t_{12}$  and  $t_{34}$  in Fig. 2.) In a similar fashion to the one used to derive (6), the holding time PDF can be approximated by the function

$$H(t) = \begin{cases} \psi(t) \exp\left(-\int_0^t \psi(x) dx\right), & t > 0, \\ 0, & t \leq 0, \end{cases} \quad (7)$$

where  $\psi(t)$  is the per unit time conditional probability of a downcrossing through  $\rho_0$  at time  $t$  given an upcrossing through  $\rho_0$  at time 0. It is straightforward to see that  $\psi(t)$  can be estimated by the following relation

$$\psi(t) = \frac{1}{\lambda_1} \int_{\rho_1=0}^{\infty} \int_{\rho_2=-\infty}^0 |\dot{\rho}_1 \dot{\rho}_2| f_{\rho_1, \rho_2, \dot{\rho}_1, \dot{\rho}_2}(\rho_0, \rho_0, \dot{\rho}_1, \dot{\rho}_2) d\dot{\rho}_1 d\dot{\rho}_2. \quad (8)$$

The next two sections present methods for evaluating  $\xi(t)$  (5) and  $\psi(t)$  (8). An exact method (Sec. III) and an approximate method (Sec. IV) are developed.

### III. EXACT EVALUATION OF $\xi(t)$ AND $\psi(t)$ : THE "CIRCLE" MODEL

The determination of the interarrival and holding time PDF's exhibits a nontrivial complexity. Whereas relations (4), (6), and (7) are trivial to evaluate, this is not the case with relations (5) and (8), which give the conditional probabilities  $\xi(t)$  and  $\psi(t)$ . The reason is that the joint PDF inside the integrals  $f_{\rho_1, \rho_2, \dot{\rho}_1, \dot{\rho}_2}(\rho_1, \rho_2, \dot{\rho}_1, \dot{\rho}_2)$  is itself difficult to evaluate.

In principle, we can obtain the above joint PDF by integration as follows

$$f_{\rho_1, \rho_2, \dot{\rho}_1, \dot{\rho}_2}(\rho_1, \rho_2, \dot{\rho}_1, \dot{\rho}_2) = \int_{\phi_1=-\infty}^{\infty} \int_{\phi_2=-\infty}^{\infty} \int_{\phi_1=0}^{2\pi} \int_{\phi_2=0}^{2\pi} f_{\rho_1, \rho_2, \dot{\rho}_1, \dot{\rho}_2, \phi_1, \phi_2, \dot{\phi}_1, \dot{\phi}_2}(\rho_1, \rho_2, \dot{\rho}_1, \dot{\rho}_2, \phi_1, \phi_2, \dot{\phi}_1, \dot{\phi}_2) d\phi_1 d\phi_2 d\dot{\phi}_1 d\dot{\phi}_2, \quad (9)$$

where the integrand is the eight-dimensional joint PDF of the amplitude  $\rho$ , its rate  $\dot{\rho}$ , the phase  $\phi$  and its rate  $\dot{\phi}$  at times 0 (subscript 1) and  $t$  (subscript 2) and is given<sup>14</sup> by

$$f_{\rho_1, \rho_2, \dot{\rho}_1, \dot{\rho}_2, \phi_1, \phi_2, \dot{\phi}_1, \dot{\phi}_2}(\dots) = \frac{\rho_1^2 \rho_2^2}{(2\pi)^4 D} \exp\left(-\frac{1}{2} \sum_{i=1}^4 \sum_{j=1}^4 (\xi_i \xi_j + \eta_i \eta_j) \sigma^{ij}\right), \quad (10)$$

where

$$\begin{aligned} \xi_1 &= x_1 & \eta_1 &= y_1 \\ \xi_2 &= x_2 & \eta_2 &= y_2 \\ \xi_3 &= \dot{x}_1 & \eta_3 &= \dot{y}_1 \\ \xi_4 &= \dot{x}_2 & \eta_4 &= \dot{y}_2 \end{aligned} \quad (11)$$

and

$$\begin{aligned} x_i &= \rho_i \cos \phi_i \\ y_i &= \rho_i \sin \phi_i \\ \dot{x}_i &= \dot{\rho}_i \cos \phi_i - \rho_i \dot{\phi}_i \sin \phi_i \\ \dot{y}_i &= \dot{\rho}_i \sin \phi_i + \rho_i \dot{\phi}_i \cos \phi_i, \end{aligned} \quad (12)$$

for  $i=1, 2$ . Here  $D$  is the determinant of  $\Sigma$ , the covariance matrix of the (Gaussian) four-dimensional PDF of the  $x$ 's (or  $y$ 's):

$$f_{x_1, x_2, \dot{x}_1, \dot{x}_2}(x_1, x_2, \dot{x}_1, \dot{x}_2) = \frac{1}{(2\pi)^2 \sqrt{D}} \exp\left(-\frac{1}{2} \sum_{i=1}^4 \sum_{j=1}^4 \xi_i \xi_j \sigma^{ij}\right)$$

and  $\sigma^{ij}$  is the  $(i, j)$ th element of  $\Sigma^{-1}$ .

Using this formula, (9) can be reduced to a single integral, with  $\tau = \phi_1 - \phi_2$  being the integration variable.<sup>14</sup>  $\xi(t)$  and  $\psi(t)$  can then be obtained by two more integrations, over  $\dot{\rho}_1$  and  $\dot{\rho}_2$ , from (5) and (6), respectively. Thus the exact evaluation of each of  $\xi(t)$  and  $\psi(t)$  involves the execution of a total of three nested numerical integrations. Reference 14 provides a detailed discussion of the behavior of the  $\xi(t)$  and  $\psi(t)$  curves predicted by the exact model. It is seen there that all  $\xi(t)$  and  $\psi(t)$  curves exhibit the same behavior for  $t$  large enough, reaching the limiting value of  $\xi(t) = \psi(t) = \lambda_1 =$  unconditional probability rate of detection, for  $t \rightarrow \infty$ .

In practice, this limit is reached for a value of time between  $3/2\pi\nu$  and  $4/2\pi\nu$  ( $\nu$  in Hz) for all threshold levels examined. These values are the decorrelation times for the corresponding thresholds. For  $t \rightarrow 0$  we have  $\xi(t)$  and  $\psi(t) \rightarrow 0$ . Section VI will show us how well the exact model compares with the data available to us, and also whether it could be substituted by the approximate model to be developed in the following section, or even by the currently used  $(\lambda, \sigma)$  model.

#### IV. APPROXIMATE EVALUATION OF $\xi(t)$ AND $\psi(t)$ : THE "SQUARE" MODEL

The analysis of Sec. III has provided some hints about the possible computational difficulties that the implementation of the exact model would bring up. This has given us the initiative to try to formulate an approximation to that model, possibly by replacing the "exact" definition of detection by some other suitable detection criterion. Denoting as before the quadrature components of  $\rho$  by  $x = \rho \cos\phi$ ,  $y = \rho \sin\phi$ , our original, exact detection criterion means that the vector  $\rho$  crosses *outwards* the periphery of a circle of radius  $\rho_0$  in the  $x$ - $y$  plane [Fig. 3(a)]. We can approximate the above circle by a square of side  $2x_0$  [Fig. 3(b)]. Detection will now be redefined as a crossing outwards across the boundary of the *square* instead of the circle. We may choose  $x_0$  as a function of  $\rho_0$  using a variety of criteria,<sup>14</sup> the best of which is to fix  $x_0 = f(\rho_0)$  so that both detection criteria (square and circle) give the same unconditional probability of detection. The approximation will, of course, cause the corresponding *conditional* probabilities to be generally different. A method for estimating these conditional probabilities will be presented here for the case of the "square" boundary.

Let  $A, B, C, D$  be the four sides of the square [Fig. 3(b)] and let us define the four (mutually exclusive) events  $A_t, B_t, C_t, D_t$  to signify the outward-crossing of the vector  $\rho$  at the corresponding edge, within  $(t, t + dt)$ . Therefore detection at  $(t, t + dt)$  is the event  $(A_t + B_t + C_t + D_t)$  with "+" denoting "or" in probability language. For the unconditional probability of detection in  $(t, t + dt)$ , we have  $dP = \lambda_1 dt = \text{prob}(A_0 + B_0 + C_0 + D_0) = 4 \text{prob}(A_0)$ . It is straightforward to show<sup>14</sup> that, in terms of  $x_0$ ,  $\lambda_1$  can be given by the following formula

$$\lambda_1 = (2\nu/\pi)[2\Phi(x_0/\sigma_1) - 1] \exp(-x_0^2/2\sigma_1^2), \quad (13)$$

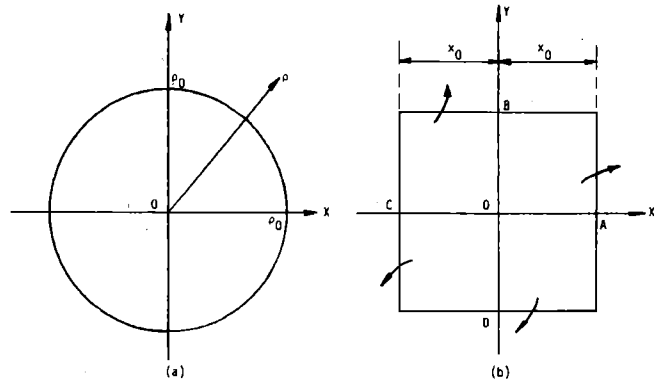


FIG. 3. Exact and approximate detection criteria.

where  $\Phi(z)$  is the standardized cumulative normal density function.

For the conditional probability  $\xi(t)dt$  of a detection in  $(t, t + dt)$  given a detection in  $(0, dt)$  we have

$$\begin{aligned} \xi(t)dt &= \text{prob}[(A_t + B_t + C_t + D_t) | (A_0 + B_0 + C_0 + D_0)] \\ &= \text{prob}(A_0 \cdot A_t + A_0 \cdot B_t + A_0 \cdot C_t + A_0 \cdot D_t) / \text{prob}(A_0), \end{aligned} \quad (14)$$

with "." denoting "and" in probability language. Then  $\xi(t)dt = \text{prob}(A_t | A_0) + \text{prob}(B_t | A_0) + \text{prob}(C_t | A_0) + \text{prob}(D_t | A_0)$  and since contributions from  $B$  and  $D$  in  $(t, t + dt)$  have to be equal (if  $\rho$  crosses edge  $A$  at  $t=0$ ) due to the existing symmetry of our configuration, we have

$$\xi(t)dt = \text{prob}(A_t | A_0) + 2 \text{prob}(B_t | A_0) + \text{prob}(C_t | A_0). \quad (15)$$

The various events in (15) are mathematically defined as follows (with subscripts 1 and 2 referring to times 0 and  $t$ , respectively)

$$\begin{aligned} A_0 &: x_1 = x_0; \dot{x}_1 \geq 0; |y_1| \leq x_0; \\ A_t &: x_2 = x_0; \dot{x}_2 \geq 0; |y_2| \leq x_0; \\ B_t &: y_2 = x_0; \dot{y}_2 \geq 0; |x_2| \leq x_0; \\ C_t &: x_2 = -x_0; \dot{x}_2 \leq 0; |y_2| \leq x_0. \end{aligned}$$

Taking each term separately, and knowing that  $\text{prob}(A_0) = \lambda_1 dt/4$ , we have

$$(i) \text{prob}(A_t | A_0) = \frac{4dt}{\lambda_1} \int_{x_2=0}^{\infty} \int_{x_1=0}^{\infty} x_1 x_2 f_{x_1, x_2, \dot{x}_1, \dot{x}_2}(x_0, x_0, \dot{x}_1, \dot{x}_2) d\dot{x}_1 d\dot{x}_2 \int_{-x_0}^{x_0} \int_{-x_0}^{x_0} f_{y_1, y_2}(y_1, y_2) dy_1 dy_2, \quad (16)$$

$$(ii) \text{prob}(B_t | A_0) = \frac{4dt}{\lambda_1} \int_{x_2=-x_0}^0 \int_{x_1=0}^{\infty} f_{x_1, x_2, \dot{x}_1, \dot{x}_2}(x_0, x_2, \dot{x}_1, \dot{x}_2) d\dot{x}_1 d\dot{x}_2 \int_{y_1=-x_0}^0 \int_{y_2=0}^{\infty} \dot{y}_2 f_{y_1, y_2, \dot{y}_2}(y_1, x_0, \dot{y}_2) dy_1 d\dot{y}_2, \quad (17)$$

$$(iii) \text{prob}(C_t | A_0) = \frac{4dt}{\lambda_1} \int_{x_2=-\infty}^0 \int_{x_1=0}^{\infty} \dot{x}_1 \dot{x}_2 f_{x_1, x_2, \dot{x}_1, \dot{x}_2}(x_0, x_0, \dot{x}_1, \dot{x}_2) d\dot{x}_1 d\dot{x}_2 \int_{y_1=-x_0}^0 \int_{y_2=-x_0}^0 f_{y_1, y_2}(y_1, y_2) dy_1 dy_2. \quad (18)$$

The detailed evaluation of the above integrals can be found in Ref. 14.

Let us now examine the modifications required for the evaluation of the conditional probability rate of an incrossing in  $(t, t + dt)$  given an outcrossing in  $(0, dt)$ , which we have denoted by  $\psi(t)$ . We have

$$\psi(t)dt = \text{prob}(A'_t | A_0) + 2 \text{prob}(B'_t | B_0) + \text{prob}(C'_t | A_0) \quad (19)$$

in complete analogy with (15), the only difference being that the primed events in (19) refer to inward crossings (incrossings) (at time  $t$ ) rather than outward crossings.

Here the events are defined as follows:

$$\begin{aligned} A_0 : x_1 = x_0; \dot{x}_1 \geq 0; |y_1| \leq x_0, \\ A'_t : x_2 = x_0; \dot{x}_2 \leq 0; |y_2| \leq x_0, \\ B'_t : y_2 = x_0; \dot{y}_2 \leq 0; |x_2| \leq x_0, \\ C'_t : x_2 = -x_0; \dot{x}_2 \geq 0; |y_2| \leq x_0. \end{aligned}$$

Then

$$(iv) \text{ prob}(A'_t | A_0) = \frac{4dt}{\lambda_1} \int_{x_2=-x_0}^0 \int_{x_1=0}^{\infty} |\dot{x}_1 \dot{x}_2| f_{x_1, x_2, \dot{x}_1, \dot{x}_2}(x_0, x_0, \dot{x}_1, \dot{x}_2) d\dot{x}_1 d\dot{x}_2 \int_{-x_0}^{x_0} \int_{-x_0}^{x_0} f_{y_1, y_2}(y_1, y_2) dy_1 dy_2, \quad (20)$$

$$(v) \text{ prob}(B'_t | A_0) = \frac{4dt}{\lambda_1} \int_{x_2=-x_0}^0 \int_{x_1=0}^{\infty} \dot{x}_1 f_{x_1, x_2, \dot{x}_1}(x_0, x_2, \dot{x}_1) d\dot{x}_1 dx_2 \int_{y_1=-x_0}^{x_0} \int_{y_2=-\infty}^0 |\dot{y}_2| f_{y_1, y_2, \dot{y}_2}(y_1, x_0, \dot{y}_2) dy_1 d\dot{y}_2, \quad (21)$$

$$(vi) \text{ prob}(C'_t | A_0) = \frac{4dt}{\lambda_1} \int_{x_2=0}^{\infty} \int_{x_1=0}^{\infty} \dot{x}_1 \dot{x}_2 f_{x_1, x_2, \dot{x}_1, \dot{x}_2}(x_0, -x_0, \dot{x}_1, \dot{x}_2) d\dot{x}_1 d\dot{x}_2 \int_{-x_0}^{x_0} \int_{-x_0}^{x_0} f_{y_1, y_2}(y_1, y_2) dy_1 dy_2. \quad (22)$$

In the computer programs developed we took advantage of the similarities of Eqs. (16)–(18) to Eqs. (20) and (22), to eliminate all redundant calculations with considerable savings in program length, memory space, and more important, computer time.

There seems to be no universal criterion that will give us the  $x_0$  that corresponds to a given  $\rho_0$ . The criterion that seems to be more reasonable to us is that of equal unconditional probabilities for the two detection boundaries. Approaches for resolving this problem are examined in Ref. 14.

A detailed study of the behavior of the  $\xi(t)$  and  $\psi(t)$  curves for the approximate model is presented in Ref. 14. It is seen there that in all cases the curves exhibit the expected asymptotic behavior for small and large times and agree closely with the exact formulation.

## V. DERIVATION OF AN "EQUIVALENT" $\lambda$ FOR THE $(\lambda, \sigma)$ MODEL

Sonar acoustic fluctuations are often discussed and approximately evaluated in terms of a particular model, called the  $(\lambda, \sigma)$  (or jump) model. This model is used because it is relatively simple and familiar, yet it is not necessarily the most realistic or the best one for any particular issue.<sup>2</sup> Its widespread use is, among other things, due to the difficulty of obtaining data which would permit more exact predictions of sonar behavior, and to the lack of exact and more rigorous theoretical treatments of the detection process. An interesting issue therefore is how the  $(\lambda, \sigma)$  model compares with the detection models developed in this paper.

In order to be able to compare the  $(\lambda, \sigma)$  model with our models, we first develop some equivalence criteria so that we evaluate these models on a common basis. In that respect, we proceed to answer the question of what values of  $\lambda$  and  $\sigma$  should be used so that such a comparison is meaningful. We do this as follows:

The basic assumption of the  $(\lambda, \sigma)$  model is that "detection opportunities" are generated in time ac-

ording to a Poisson process of parameter  $\lambda$ .<sup>1</sup> The reciprocal of  $\lambda$  is known as the "relaxation time" of the process and its value is usually taken arbitrarily from empirical considerations of the process, and without any explicit relationship to the detection threshold level. At any particular detection opportunity, a detection occurs if the level  $\Lambda$  in dB, which is assumed to be normally distributed with a mean and a standard deviation defined in Ref. 7, exceeds a specified threshold level  $\Lambda_0$ . It can be shown<sup>7</sup> that the theoretical value of  $\sigma$  is always equal to 5.6 dB, in a saturated phase random regime as we have assumed, hence the exclusive use of this value in all considerations of the  $(\lambda, \sigma)$  model.

In order to put the above defined  $(\lambda, \sigma)$  model into a common basis of comparison with our detection models, we estimate, in terms of its parameters, the per unit time unconditional probability of detection as follows:

The probability that any particular "detection opportunity" will end up in a detection is  $\alpha = \text{prob}(\Lambda \geq \Lambda_0)$ . Since  $\Lambda = 10 \log_{10} \rho^2$ ,  $\Lambda_0 = 10 \log_{10} \rho_0^2$  and  $\rho$  is Rayleigh distributed, we have that  $\alpha = \text{prob}(\rho \geq \rho_0)$  or

$$\alpha = \exp(-\rho_0^2/2\sigma_1^2).$$

Under the assumption of mutual independence among the values of  $\Lambda$  at consecutive detection opportunities, it is straightforward to show that detection events in the  $(\lambda, \sigma)$  model are generated in time according to another Poisson process, of parameter  $\lambda_2 = \alpha\lambda$ ;  $\lambda_2$  is then the per unit time unconditional probability of detection for the  $(\lambda, \sigma)$  model.

A common basis of comparison between the  $(\lambda, \sigma)$  model and our detection models implies that  $\lambda_2 = \lambda_1$ , hence from (4) and (23) we have

$$\lambda \exp(-\rho_0^2/2\sigma_1^2) = [\rho_0 \cdot \nu/\sigma_1 (2\pi)^{1/2}] \exp(-\rho_0^2/2\sigma_1^2),$$

or

$$\lambda = [\nu\rho_0/\sigma_1 (2\pi)^{1/2}]. \quad (24)$$

The above value of  $\lambda$  is called "equivalent  $\lambda$ ." It is the

value that  $\lambda$  should take in the  $(\lambda, \sigma)$  model so that this model exhibits an average number of detections per unit time which is consistent with the values of  $\rho_0$ ,  $\sigma_1$ , and  $\nu$ . If this is the case, the "equivalent"  $(\lambda, \sigma)$  model has the same average number of detections per unit time with our new detection models. All comparisons of the  $(\lambda, \sigma)$  model with our models implicitly assume that  $\lambda$  takes the above value. Note that while (24) agrees to what has been a widespread qualitative belief that " $\lambda$  should be proportional to  $\nu$ ," it also states that  $\lambda$  should also be connected with the specified detection threshold level  $\rho_0$  as well as the standard deviation  $\sigma_1$  of  $\rho$ .

Since the detection process in the  $(\lambda, \sigma)$  model is itself Poisson, the PDF for the time between two successive detections (interarrival time) is negative exponential, of the form

$$f_i(t) = \lambda_2 \exp(-\lambda_2 t), \quad t \geq 0, \quad (25)$$

with

$$\lambda_2 = \alpha \cdot \lambda = \lambda_1.$$

The key assumption of the  $(\lambda, \sigma)$  model is the absence of time correlation between signals. This "no-memory" property leads to analytic simplicity, but conceivably also to discrepancies between theory and experimental data. Moreover, physical and statistical reasoning and evidence suggest that a time correlation between the signals does exist. Thus the intensity of the signal at a particular instant cannot be independent of the intensity of that signal a few moments ago, as the  $(\lambda, \sigma)$  model assumes.

A summary of the properties of the  $(\lambda, \sigma)$  model, in terms of our previously defined terminology, follows

(a)  $\xi(t) = \psi(t) = \text{const.} = \lambda_2,$

(b) PDF for interarrival time: Negative exponential, given by Eq. (25),

(c) PDF for holding time: This PDF must be such that the sum of the two random variables  $x_1 = t_2 - t_1$  and  $x_2 = t_3 - t_2$ , (where  $t_1 =$  time of first upcrossing,  $t_2 =$  time of first downcrossing,  $t_3 =$  time of second upcrossing), must follow the negative exponential distribution (Eq. 25). If we assume  $x_1$  and  $x_2$  to be mutually independent, the PDF of their sum must be the convolution of their

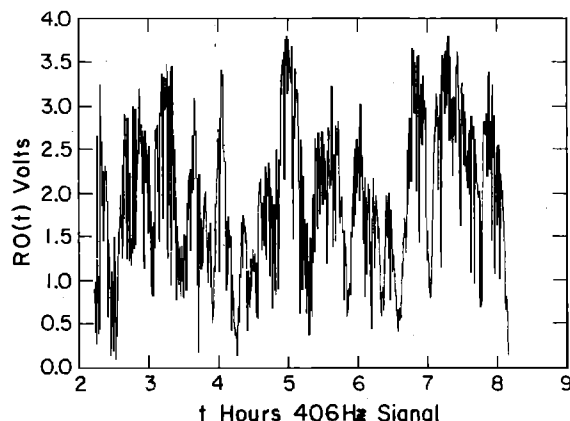


FIG. 4. WHOI 447 record (truncated), time series of  $\rho(t)$ .

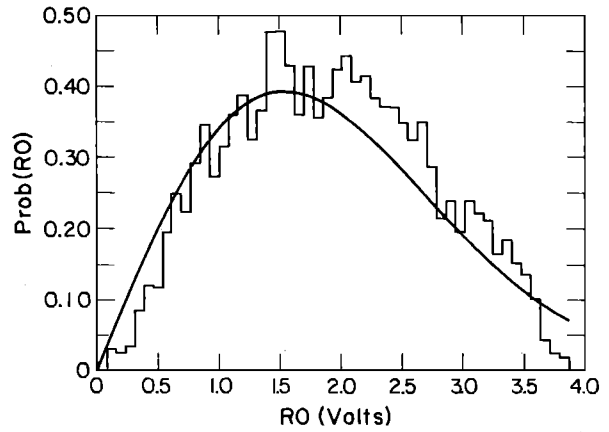


FIG. 5. WHOI 447 record (truncated), histogram of  $\rho(t)$ .

PDF's. It then follows that the PDF of  $x_1$  must be a one-half-order Erlang (or Gamma) PDF given by the expression

$$f_{x_1}(x_1) = (\lambda_2 / \pi x_1) e^{-\lambda_2 x_1}. \quad (26)$$

## VI. RESULTS OF THE DATA ANALYSIS

Our first set of data (referred to from now on as the WHOI data) was obtained from an experiment performed by Porter and Spindel near Eleuthera,<sup>15</sup> and was made available by the Woods Hole Oceanographic Institution. The data was recorded during a long range acoustic propagation experiment. It consists of three records in which two signals per record, one at 220 and one at 406 Hz, were transmitted from Eleuthera to drifting sonobuoys approximately 300 km northeast towards Bermuda. A Doppler position-tracking system was used to remove mean multipath phaserates due to sonobuoy motions. This data was previously analyzed by Dyer and Shepard,<sup>4</sup> Hamblen,<sup>5</sup> and Mikhalevsky.<sup>7-9</sup>

The second set of data (referred to from now on as the CASE data) was obtained from the records of the CASE experiment whose description can be found in Ref. 16. In this experiment three configurations were used: (1) fixed source on a seamount, (2) source towed by a

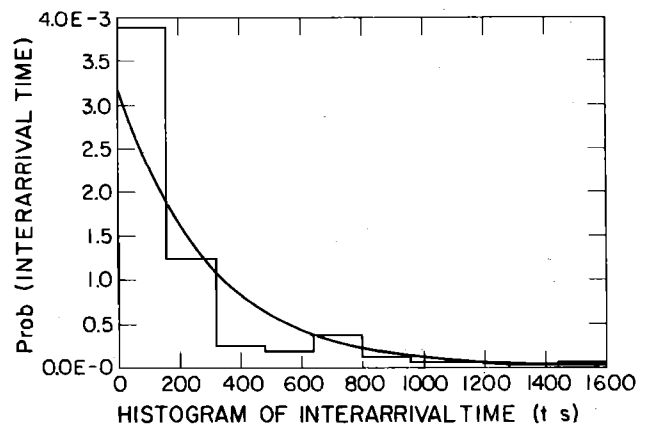


FIG. 6. WHOI 447, level  $\rho_0 = \sigma_1$ , histogram versus  $(\lambda, \sigma)$ , interarrival time.

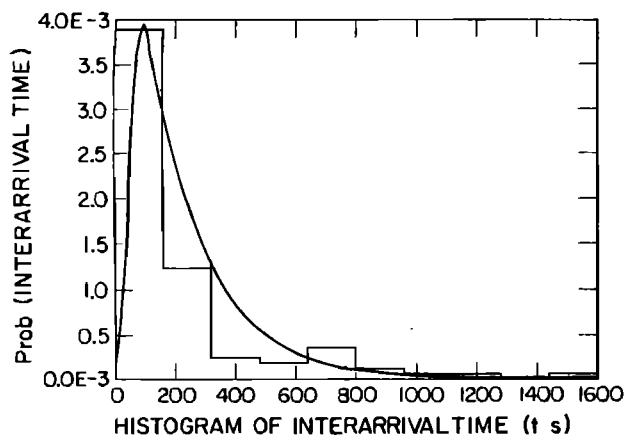


FIG. 7. WHOI 447, level  $\rho_0 = \sigma_1$ , histogram versus "square," interarrival time.

surface ship, and (3) source mounted on a submersible. The signals were monitored at four widely separated fixed deep water receivers at ranges varying from 200 to 400 km. Two carrier frequencies were employed, one at 15 and another at 33 Hz. More about the CASE data base can be found, besides the basic source,<sup>16</sup> in Ref. 17.

We have analyzed both groups of data available to us with a multipurpose, interactive data analysis computer program, developed specifically for that purpose.<sup>14</sup> For a given data record, this program can either plot  $\rho(t)$  and perform the analysis for the whole length of the record, or *isolate* the part of it that exhibits a behavior compatible with our assumption, namely fully developed saturated phase random propagation<sup>5,8</sup> and analyze only that portion of it. The matching of the data with the predicted PDF's of interarrival and/or holding times from the above models is checked by performing a  $\chi^2$  goodness-of-fit test at the 0.05 level of significance.<sup>18</sup>

#### A. The WHOI data

The WHOI data is far from ideal for comparison with our models. As Hamblen<sup>5</sup> points out, it may be true that most of the records satisfy the multipath phase

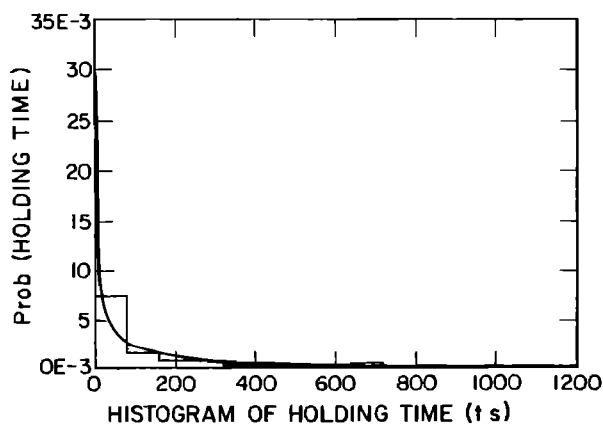


FIG. 8. WHOI 447, level  $\rho_0 = \sigma_1$ , histogram versus  $(\lambda, \sigma)$ , holding time.

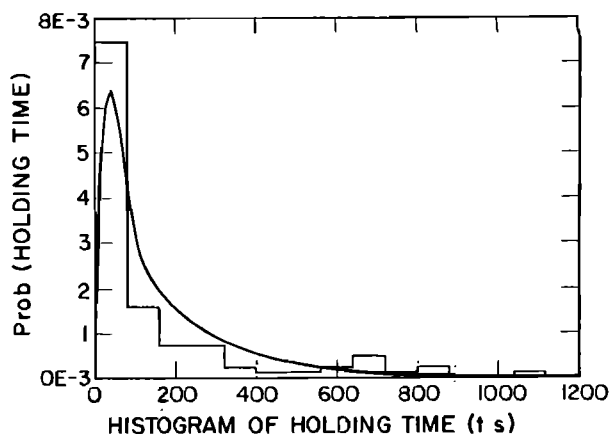


FIG. 9. WHOI 447, level  $\rho_0 = \sigma_1$ , histogram versus "square," holding time.

randomness assumption, but we cannot be so confident about their stationarity. In a brief analysis<sup>5</sup> it is seen that  $\nu^2$  seems to be quite stationary, whereas  $\sigma_1^2$  is not, fluctuating (in a single record) over a range of more than six standard deviations. By comparison,  $\nu^2$  rarely fluctuates over two standard deviations. This relative instability of  $\sigma_1^2$  can be checked by comparing the histogram of  $\rho$  with its theoretical (Rayleigh) PDF. Hamblen presents plots of this histogram for all WHOI records, from which one can see, both visually and by observing the  $\chi^2$ -test results, that the data agrees very poorly with the expected forms of the  $\rho$  PDF. Other random variables, not strongly influenced by the nonstationarity of  $\sigma_1^2$ , behave much better (e.g., phase, phase rate, etc). However, since our detection models are primarily concerned with the  $\rho$  PDF, we decided to present the record that exhibited the best overall fit in that PDF. This turned out to be record 447 with frequency  $f = 406$  Hz. (In fact, we analyzed only the portion of this record that looked sufficiently stationary.) The time series appears in Fig. 4, and the histogram in Fig. 5. One can notice the rather poor fit of the Rayleigh PDF to the histogram of  $\rho$ . For this record  $\sigma_1^2 = 2.388 \text{ V}^2$  and  $\nu = 0.00309$  Hz; these estimates were used as inputs in all detection models, and were obtained from Refs. 5-8.

TABLE I. Results of the WHOI data, record 447 carrier frequency 406 Hz,  $\sigma_1^2 = 2.388 \text{ V}^2$  and  $\nu = 0.00309$  Hz. The PDF's given by the  $(\lambda, \sigma)$  and approximate square model are compared with the histogram for a threshold level  $\rho_0 = \sigma_1 = 1.15 \text{ V}$ . For the square model,  $x_0 \approx 1.2\rho_0$ . The  $\chi^2$  goodness-of-fit test is performed and is successful when  $\chi^2 < \chi^2_{\alpha}$ .

PDF	Model	Mode (s)	Mean (s)	$\chi^2$	$\chi^2_{\alpha}$	Fig. No.
Interarrival time	Observed	70	228	...	...	6, 7
	$(\lambda, \sigma)$	0	313	13.37	12.59	6
	Square	80	245	29.50	11.07	7
Holding time	Observed	40	161	...	...	8, 9
	$(\lambda, \sigma)$	0	166	18.68	14.07	8
	Square	40	173	36.23	15.51	9

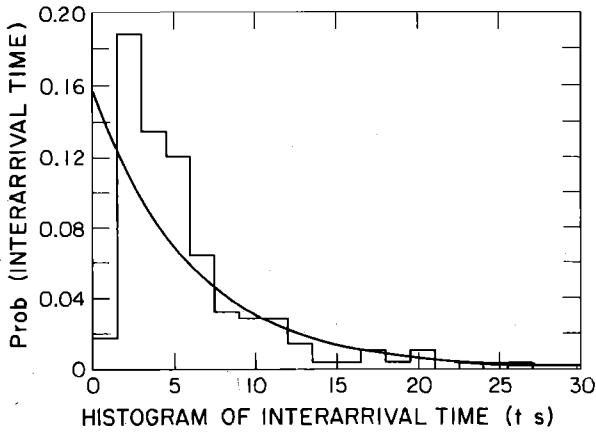


FIG. 10. CASE 21 record, level  $\rho_0 = \sigma_1$ , histogram versus  $(\lambda, \sigma)$  interarrival time.

Some of the results of the data analysis for the above record are presented in Figs. 6–9 and in Table I. The threshold level selected was  $\rho_0 = 1.15$  V. The value of  $x_0$  for the “square” model was chosen so as to give equal unconditional probability of detection with the “circle” model ( $x_0 \approx 1.2 \rho_0$ ). Figure 6 displays a comparison of the interarrival time predicted by the  $(\lambda, \sigma)$  model (with the “equivalent” value of  $\lambda$  used) with the data. The fit appears to be fair, yet seems inferior to the fit in Fig. 7, which shows a comparison of the interarrival time predicted by the “square” model with the data. One should particularly notice the difference in the height of the peak values of the PDF’s between these two figures. The “square” model is in much closer agreement with the data in that respect.

The apparent superiority of the “square” model is shown more clearly in the holding time comparison (Figs. 8 and 9). Figure 8 displays the  $(\lambda, \sigma)$  model’s one-half-order Erlang holding time PDF and Fig. 9 the “square” model’s holding time PDF versus the data.

Various statistics of the specific runs mentioned above are displayed in Table I. These refer to the most probable interarrival and holding times (mode), to the average interarrival and holding times (mean), and to statistics obtained after applying the  $\chi^2$  goodness-

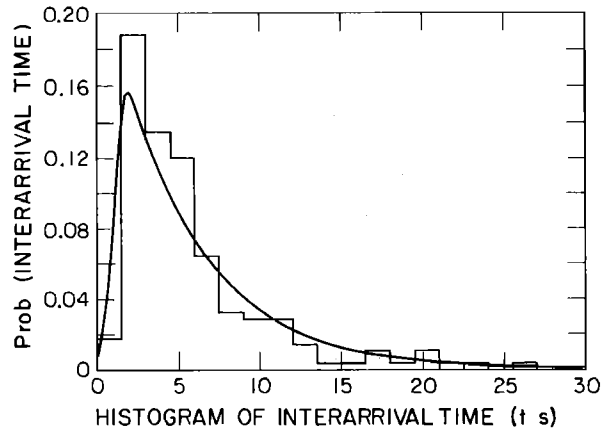


FIG. 12. CASE 21 record, level  $\rho_0 = 1.75\sigma_1$ , histogram versus “square,” interarrival time. ( $x_0$  computed so as to produce the same unconditional probability with that of the circle model.)

of-fit test. One can observe the following: First, the  $(\lambda, \sigma)$  model is totally unrealistic in predicting the modes of the interarrival and holding times, setting them to zero, while the “square” model compares very well with the data in that respect. Second, the  $(\lambda, \sigma)$  model highly overpredicts the mean interarrival time and slightly overpredicts the mean holding time. The “square” model overpredicts both mean times as well, being closer to the data for the interarrival time case. Third, all runs fail the  $\chi^2$  test. This outcome is perhaps not a surprise, given the nonimpressive fit of Fig. 5 (likely due to nonstationarities of the data) and the certainly nonoutstanding fits of Figs. 6–9.

## B. The CASE data

In this paper we present results from the analysis of one record of the CASE data, record 21. Although a record of low signal-to-noise ratio, record 21 is one of the few CASE records that satisfy the phase-randomness assumption, at a far greater extent than the WHOI data; most of the other records are nonstationary. Given the fact that this record has a low signal-to-noise ratio, our comparison as far as detection is con-

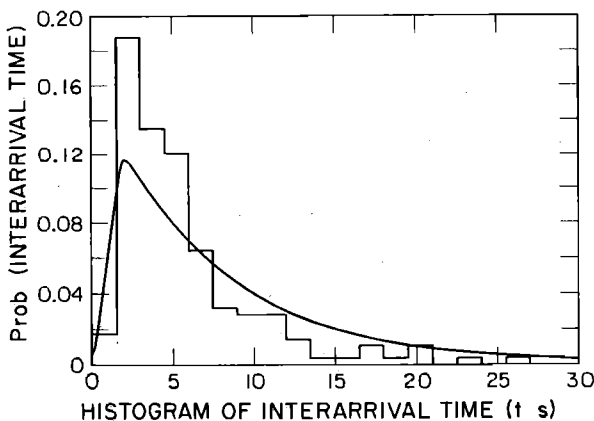


FIG. 11. CASE 21 record, level  $\rho_0 = 1.75\sigma_1$ , histogram versus “square,” interarrival time ( $x_0 = \rho_0$ ).

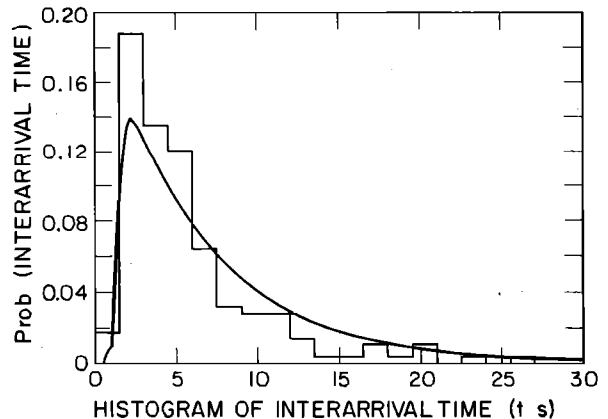


FIG. 13. CASE 21 record, level  $\rho_0 = 1.75\sigma_1$ , histogram versus “circle,” interarrival time.

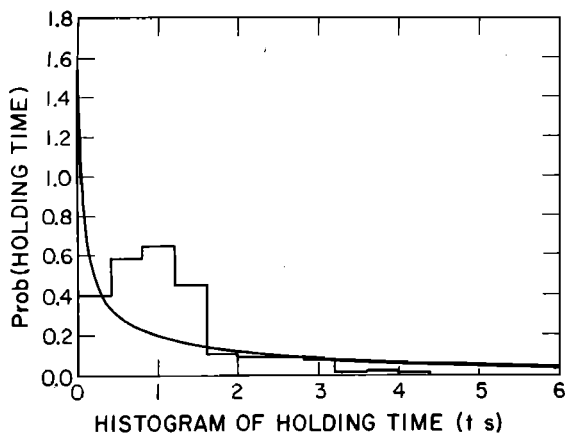


FIG. 14. CASE 21 record, level  $\rho_0 = 1.75\sigma_1$ , histogram versus  $(\lambda, \sigma)$ , holding time.

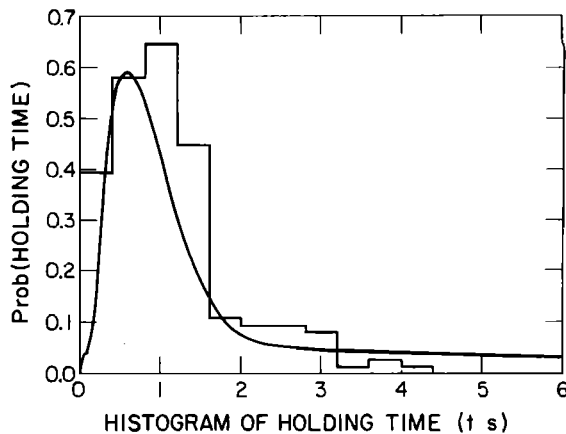


FIG. 15. CASE 21 record, level  $\rho_0 = 1.75\sigma_1$ , histogram versus "square," holding time.

cerned is likely to have limited practical significance. However, we decided to present it since the record itself satisfies the phase-randomness assumption on which our detection models are based. The results of this comparison are presented in Figs. 10–15 and in Table II. The parameters of record 21 are carrier frequency 15 Hz,  $\sigma_1^2 = 15.9 V^2$ ,  $\nu = 0.173$  Hz.

The "circle" model and two versions of the "square" model were tested for that record. In all cases,  $\rho_0 = 1.75\sigma_1 = 7$  V. Specifically the following comments are in order:

Figure 10 shows how the  $(\lambda, \sigma)$  model (with the "equivalent" value of  $\lambda$  used) compares with the data (interarrival time). One can clearly observe the inability of this model to predict the very low probability of a very short interarrival time, which seems to be confirmed by the data. This is to be contrasted with Figs. 11–13, which compare our detection models with the data (also for interarrival time). In Fig. 11, the "square" model is used, with  $x_0 = \rho_0$ . In Fig. 12, the "square" model is also used, but this time with  $x_0$  chosen such that the "square" model gives the same unconditional probability of detection with the "circle" model. Figure 13 dis-

plays the interarrival time PDF of the "circle" model. It can be seen that the "square model, with  $x_0$  chosen as in Fig. 12 represents a very good approximation of the "circle" model.

Figure 14 displays the holding time PDF of the  $(\lambda, \sigma)$  model versus the data. The fit appears to be very poor, in contrast to that of Fig. 15, where the holding time PDF of the "square" model is compared with data.

Table II summarizes statistics for the above runs. It can be seen again that the new detection models give generally better predictions for the modes and means of the interarrival and holding times. This table shows that again all runs fail the  $\chi^2$  test, although certainly to a far less extent than the WHOI data. The reasons for this outcome are still unclear, and are conceivable to lie in issues regarding sufficient sample size.

## VII. DISCUSSION

Two new detection models were developed under the assumption of phase-random multipath ocean acoustic fluctuations. The methodology developed in this paper is not bound by the phase-randomness assumption; it is equally valid for any other explicitly specified random

TABLE II. Results of CASE record 21, carrier frequency 15 Hz,  $\sigma_1^2 = 15.9 V^2$ ,  $\nu = 0.173$  Hz, and  $\rho_0 = (1.75\sigma_1) = 7$  V. For the square (mod) case the value of  $x_0$  was set equal to  $\rho_0$ , for all other applications of the square model reported in this paper  $x_0$  was computed so as to produce the same unconditional probability with that of the circle model. The  $\chi^2$  goodness-of-fit test is performed and is successful when  $\chi^2 < \chi_g^2$ .

PDF	Model	Mode (s)	Mean (s)	$\chi^2$	$\chi_g^2$	Fig. No.
Interarrival time	Observed	2.4	4.2	...	...	
	$(\lambda, \sigma)$	0.0	4.8	69.43	19.68	10
	Square (mod)	2.1	4.7	44.68	22.36	11
	Square	2.1	4.5	29.99	21.03	12
Holding time	Circle	2.4	5.5	21.79	19.68	13
	Observed	1.0	1.1	...	...	14, 15
	$(\lambda, \sigma)$	0.0	2.4	171.81	21.03	14
	Square	0.6	1.2	56.73	18.31	15

process. In that respect, it would be interesting to try to develop detection models for other known fluctuation processes.

The main conclusion from this study is that *the detection process has memory*. In that respect, a detection now will very strongly influence the probability of another detection at some time in the immediate future. Both our theoretical models as well as the overwhelming majority of the data have shown that it is very unlikely to have two detections separated by a very short time interval. On the other hand, two detections separated by a sufficiently long time interval are essentially uncorrelated. The decorrelation interval is, in general, a rather weak function of the selected threshold level  $\rho_0$ , yet it is always of the order of  $0.4/\nu$  to  $0.6/\nu$  (in seconds where  $\nu$  is in Hz).

Both our exact and approximate models agree with the above. The  $(\lambda, \sigma)$  model, when used with the appropriate "equivalent  $\lambda$ ," exhibits a satisfactory behavior for large enough times, yet is unable, being memoryless, to correctly predict the detection probability immediately after a detection. Therefore, depending upon the magnitude of our time intervals with respect to the decorrelation time, the  $(\lambda, \sigma)$  behavior may (for long enough times) or may not (for short times) hold.

Our models were further tested by the examination of the value of certain easy-to-obtain statistics of the PDF's. In particular, the most probable time (mode) and the mean interarrival and holding times were computed. From the results presented in Tables I and II we conclude that the  $(\lambda, \sigma)$  model makes poor predictions of the mode (which is always zero for both interarrival and holding time), whereas our models and the data examined suggest numbers in the ranges of  $0.4/\nu$  to  $0.3/\nu$  for the interarrival time and  $0.2/\nu$  to  $0.1/\nu$  for the holding time. If  $\nu$  is small enough, therefore, the  $(\lambda, \sigma)$  predictions are quite inaccurate. Concerning the mean interarrival and holding times, our model predictions are in better agreement with the observed values than the predictions of the  $(\lambda, \sigma)$  model.

From a practical point of view, the value of the developed models lies in one's increased ability to *predict the timing* of events associated with detection, an ability which is seriously limited under the no-memory assumption of the  $(\lambda, \sigma)$  model. For instance, now one can estimate *when* the signal will go below the threshold, given that it has exceeded it at some particular instant; *when* the signal is going to cross that threshold again; plus, other statistics related to the interarrival and holding times, such as their mean and most probable values. The additional knowledge associated with these models is believed to enhance the overall understanding of the mechanisms of detection in the ocean and may also be used as a stepping stone for more ad-

vanced processing of signals, including scenarios in which the signals are nonstationary, i. e.,  $\sigma_1^2$  and  $\nu^2$  are functions of time.

## ACKNOWLEDGMENTS

This work was supported by the Office of Naval Research under Contract No. N00014-79-C-0238. We are particularly indebted to Ira Dyer for his continuous assistance and suggestions. We would also like to thank Tom Fortmann, Yaakov Bar-Shalom, Molly Scheffe, and Bill Hamblen for their comments, as well as Neil Miller and Robert Spindell for providing the data with which our models were tested. Finally, thanks are due to Jim Smith for the guidance and administrative support he provided to the project.

- <sup>1</sup>B. J. Mc Gabe and B. Belkin, "A Comparison of Detection Models Used in ASW Operations Analysis," Daniel H. Wagner Associates, Paoli, PA (1973).
- <sup>2</sup>J. D. Kettle, "Current State of Sonar Variability Analysis," in "O. R. Models of Fluctuations Affecting Sonar Detection" (Workshop held at DTNSRDC, 1975).
- <sup>3</sup>I. Dyer, J. Acoust. Soc. Am. **48**, 337-345 (1970).
- <sup>4</sup>I. Dyer and G. W. Shepard, J. Acoust. Soc. Am. **61**, 937-942 (1977).
- <sup>5</sup>W. R. Hamblen, "Phase Random Multipath Model for Acoustic Signal Fluctuation in the Ocean and its Comparison with Data," Ph.D. thesis, M.I.T. (1977).
- <sup>6</sup>P. N. Mikhalevsky, and I. Dyer, J. Acoust. Soc. Am. **63**, 732-738 (1978).
- <sup>7</sup>P. N. Mikhalevsky, J. Acoust. Soc. Am. **66**, 751-762 (1979).
- <sup>8</sup>P. N. Mikhalevsky, "The Statistics of Finite Bandwidth, Modulated Acoustic Signals Propagated to Long Ranges in the Ocean, Including Multiple Source Effects," Ph.D. thesis, M.I.T. (1979).
- <sup>9</sup>P. N. Mikhalevsky, J. Acoust. Soc. Am. **67**, 812-815 (1980).
- <sup>10</sup>H. N. Psaraftis, "Some New Aspects of Slamming Probability Theory," J. Ship Res. **22** (3) (1978).
- <sup>11</sup>M. S. Longuet-Higgins, "The Distribution of Intervals Between Zeros of a Stationary Random Function," R. Phil. Soc. Trans. **254** (1047) (1962).
- <sup>12</sup>S. O. Rice, "Mathematical Analysis of Random Noise," Bell Syst. Tech. J. **23** (1944) and **24** (1945).
- <sup>13</sup>J. A. McFadden, "The Axis-Crossing Intervals of Random Functions: II," IRE Trans. Inf. Theory, **II-4** (1958).
- <sup>14</sup>A. N. Perakis, "A New Probabilistic Detection Model for Phase Random Ocean Acoustic Fluctuations and its Comparison with Data," M.S. thesis, M.I.T., Dept. of Ocean Eng. (January 1980).
- <sup>15</sup>R. Porter and R. Spindel, J. Acoust. Soc. Am. **61**, 943-958 (1977).
- <sup>16</sup>J. N. Anton, "A Fluctuation Data Base for the CASE Experiment," Tech. Rep. 5204-2, Systems Control, Inc. (April, 1978).
- <sup>17</sup>I. Dyer, H. Psaraftis, P. Mikhalevsky, and A. Perakis, "Fluctuation Statistics and Signal Detection Modelling," Interim Report on ONR Project N0014-79-C-0238, M.I.T. (1979); M.I.T., O.E. Rep. No. 79-8.
- <sup>18</sup>J. S. Bendat and A. G. Piersol, *Random Data: Analysis and Measurement Procedures* (Wiley, New York, 1971).